Model Predictive Pulse Pattern Control with Integrated Balancing of the Neutral Point Potential

Tobias Geyer and Vedrana Spudić
ABB Corporate Research
Segelhofstrasse 1K, Baden-Dättwil, Switzerland
Email: t.geyer@ieee.org and vedrana.spudic@ch.abb.com

Keywords

≪Control of drive≫, ≪Neutral-point-clamped converter≫, ≪Non-linear control≫, ≪Optimized pulse pattern≫, ≪Variable speed drive≫.

Abstract

A neutral-point-clamped inverter operated with optimized pulse patterns is considered with an induction machine. For this setup, a control method is proposed that achieves high-bandwidth control of the electromagnetic torque and machine magnetization through stator flux trajectory tracking while balancing the inverter's neutral point (NP) potential. More specifically, a model predictive pulse pattern control problem is formulated and solved that addresses stator flux control and balancing of the NP potential in one single control loop. The proposed controller achieves minimal current distortions per switching frequency and is thus well-suited to medium-voltage power converters operating at low pulse numbers.

Introduction

Optimized pulse patterns (OPPs) are pulse width modulation (PWM) switching patterns with optimized harmonic characteristics [1, 2]. The corresponding switching angles and switching transitions are computed in an offline procedure. For inverters connected to an electrical machine, the optimization objective is typically the minimization of the total harmonic distortion (THD) of the stator currents.

The use of OPPs, however, intrinsically complicates the controller design. Unlike carrier-based PWM (CB-PWM) or space vector modulation (SVM), OPPs relinquish any fixed-length modulation interval. As a result, regularly-spaced time instants at which the current ripple is zero do not exist. Instead, the sampled current always includes its fundamental component as well as its ripple, impeding the design of closed-loop controllers. When adopting linear controllers, such as PI controllers, and the commonly-used technique of averaging, the controller must be made slow. This leads to a poor disturbance rejection and a poor performance during transients. Furthermore, the switching angles of OPPs generally exhibit discontinuities when varying the modulation index; linear controllers manipulating the modulation index thus cause large disturbances at these discontinuities. The often used approach that enables linear control designs is to enforce continuity of the switching angles with respect to the modulation index. This, however, yields OPPs with a suboptimal harmonic performance [3] and therefore should be avoided.

The recently proposed model predictive pulse pattern control (MP^{3}C) concept resolves both issues: it provides a high control bandwidth and does not impose restrictions on the design and optimality of the OPPs, allowing us to use OPPs with discontinuous switching angles [4]. The MP^{3}C method tracks an optimal stator flux reference in stationary orthogonal coordinates by manipulating the switching instants of the OPP. By controlling the stator flux vector, control of the machine's electromagnetic torque and magnetization is achieved. While operating at steady-state, minimal harmonic current distortions per switching frequency are achieved. During transients such as torque steps, a dynamic performance akin

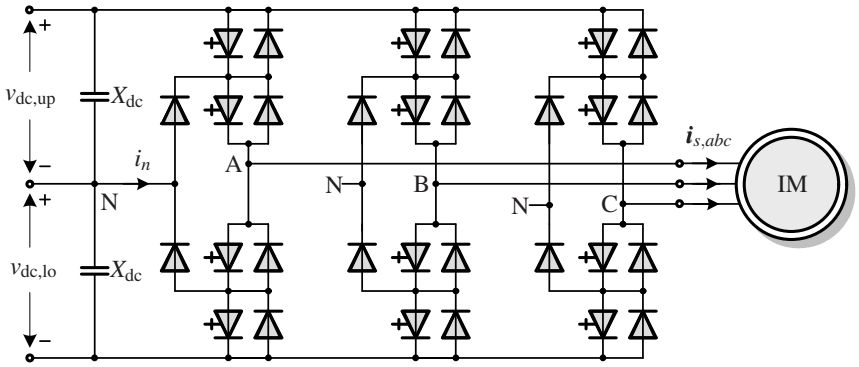

Fig. 1: Three-level neutral-point-clamped inverter driving an induction machine

to that of direct torque control is possible, provided that additional switching transitions may be inserted in the presence of large flux errors [5].

Aside from stator flux control, an additional control objective arises in neutral-point-clamped (NPC) inverters: the voltages of the upper and lower dc-link capacitors must be balanced by maintaining their difference—the neutral point (NP) potential—close to zero. Despite the natural balancing characteristic of the NPC inverter [6], active balancing techniques are commonly employed in CB-PWM and SVM schemes to facilitate a fast correction and to avoid a lasting dc offset in the NP potential. This is particularly important in medium-voltage applications, in which the ohmic resistance in the system is low [6].

Most control methods of the NP potential are based on the manipulation of the inverter's common-mode voltage. A positive bias in the common-mode voltage, for example, shifts the phase voltages towards the upper inverter half. Depending on the sign of the phase current, this adds a positive or negative offset to the current drawn from the NP [7, 8], which, in turn, modifies the NP potential. Based on this principle, a dedicated NP controller can be designed that manipulates the common-mode voltage reference that is fed to the modulator. This control method was introduced in [9] and extended in [7] and [8]. It regulates the dc offset of the NP potential to zero by manipulating the dc common-mode component; the ac (or ripple) component of the NP potential is typically not targeted. Common-mode voltage offsets can also be generated by manipulating the deadtime that is added between turn-on and turn-off transitions of the semiconductor switches [10].

On the other hand, instantaneous control of the common-mode voltage, and thus of the NP potential, can be achieved by exploiting the redundancy in the voltage vectors [11]. The inner voltage vectors form pairs, which generate the same differential-mode voltage but exhibit the opposite common-mode voltage. As a result, one of the two voltage vectors will always increase the NP potential whereas the other one will decrease it. Accordingly, in SVM, the existence of pairs of redundant voltage vectors can be exploited by varying the ratio of their *on* durations in the switching sequence [12]. This, in effect, also controls the NP potential via the common-mode voltage. Alternatively, at low output voltages, fast NP control can be achieved by shifting the entire pulse pattern either completely into the upper half or the lower half of the inverter [13].

However, the literature on balancing the NP potential in NPC inverters modulated with OPPs is scarce. One notable exception is [14], which considers a push-pull configuration for a variable-speed drive. The two series-connected NPC inverters achieve five voltage levels per phase. When mapping the five-level OPP into the two three-level OPPs for the respective NPC inverters, a degree of freedom emerges that can be exploited to control the NP potential.

This paper proposes a general method to balance the NP potential in NPC inverters when using OPPs by extending the MP^{3}C framework. Recall that MP^{3}C commonly uses two terms in its objective function [4]. The first term penalizes the predicted stator flux error, whereas the second term penalizes the modifications of the switching instants. To include the NP potential balancing in MP^{3}C, a third term is added to the objective function that penalizes the predicted deviation of the NP potential from its refer-

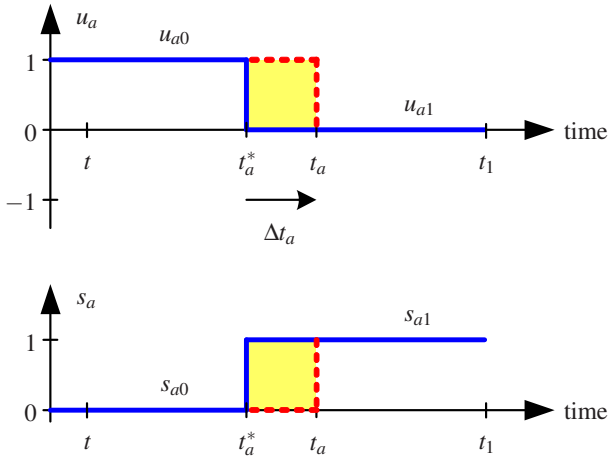

Fig. 2: Delaying the negative switching transition $\Delta u_a = -1$ in phase a by Δt_a with regard to the nominal switching time t_a^* decreases the time interval in which $u_a = 0$ is applied and thus shortens the influence of the phase a current on the NP potential

ence. To do so, a model is derived that predicts the correction of the NP potential as a function of the modifications to the switching instants within the considered prediction horizon.

Neutral-Point-Clamped Inverter

Consider an NPC voltage source inverter as shown in Fig. 1. To describe the switch positions of a phase, we introduce the integer variable $u_x \in \{-1,0,1\}$, where $x \in \{a,b,c\}$ denotes one of the three phases. The three-phase switch position is defined as $\boldsymbol{u} = [u_a\ u_b\ u_c]^T$.

Throughout this paper, we adopt a per unit (pu) system and use normalized quantities. In particular, the normalized capacitance of the upper (or lower) dc-link half is denoted by the reactance X_{dc}. The base quantities of the pu system will be defined when evaluating the performance.

The total dc-link voltage is $v_{\mathrm{dc}} = v_{\mathrm{dc,lo}} + v_{\mathrm{dc,up}}$, where $v_{\mathrm{dc,lo}}$ and $v_{\mathrm{dc,up}}$ refer to the lower and upper capacitor voltages of the dc-link. The NP potential $v_n = \frac{1}{2}\left(v_{\mathrm{dc,lo}} - v_{\mathrm{dc,up}}\right)$ is defined as half the difference between these two voltages. The NP potential evolves in accordance with the differential equation

$$\frac{d}{dt} v_n = -\frac{1}{2X_{\mathrm{dc}}} i_n\,, \tag{1}$$

where i_n denotes the NP current. A phase with the (stator) phase current i_{sx} contributes to the NP current when the switch position in this phase is zero. The NP current is, thus, given by

$$i_n = i_{sa}(1-|u_a|) + i_{sb}(1-|u_b|) + i_{sc}(1-|u_c|)\,. \tag{2}$$

We define the new binary variable

$$s_x = 1 - |u_x| = \begin{cases} 0 & \text{if } u_x \in \{-1,1\} \\ 1 & \text{if } u_x = 0 \end{cases} \tag{3}$$

in each phase $x \in \{a,b,c\}$. With this, the NP current in (2) can be written in the compact form

$$i_n = i_{sa}s_a + i_{sb}s_b + i_{sc}s_c\,. \tag{4}$$

Control Principle of the NP Potential

The NP potential at the future time instant $t_1 > t$ can be computed by inserting (4) into (1), and by integrating both sides from t to t_1

$$v_n(t_1) = v_n(t) - \frac{1}{2X_{\mathrm{dc}}} \int_t^{t_1} \big(i_{sa}(\tau)s_a(\tau) + i_{sb}(\tau)s_b(\tau) + i_{sc}(\tau)s_c(\tau)\big)\, d\tau\,. \tag{5}$$

In order to compute (5), consider first the contribution from phase a over the time interval $[t\ t_1]$

$$\Delta v_{n,a} = -\frac{1}{2X_{\mathrm{dc}}} \int_t^{t_1} i_{sa}(\tau)s_a(\tau)\, d\tau\,. \tag{6}$$

Assume that one switching transition occurs in phase a in this time interval. Let $\Delta u_a = u_{a1} - u_{a0}$ denote this switching transition, where Δu_a is a nonzero integer variable. Correspondingly, we define

$$\Delta s_a = s_{a1} - s_{a0}\,. \tag{7}$$

The nominal switching time is t_a^*, the actual or modified switching time is

$$t_a = t_a^* + \Delta t_a\,, \tag{8}$$

and Δt_a denotes the switching instant modification, see Fig. 2 for an illustrating example.

Owing to our assumption that one switching transition occurs in phase a within the time interval $[t\ t_1]$, (6) can be rewritten as

$$\Delta v_{n,a} = -\frac{1}{2X_{\mathrm{dc}}} i_{sa}(t) \Big(\int_t^{t_a} s_{a0}\, d\tau + \int_{t_a}^{t_1} s_{a1}\, d\tau \Big)\,, \tag{9}$$

where we have assumed that the phase a stator current i_{sa} is constant over the time interval $[t\ t_1]$. With the help of (7) and (8), (9) can be reformulated as

$$\Delta v_{n,a} = -\frac{1}{2X_{\mathrm{dc}}} i_{sa}(t) \Big(s_{a0}(t_1 - t) + \Delta s_a t_1 - \Delta s_a t_a^* - \Delta s_a \Delta t_a \Big)\,. \tag{10}$$

As can be seen, the phase a contribution to the NP potential at time t_1 can be manipulated through the last term in (10), using the switching time modification Δt_a. We interpret this last term as a correction to the NP potential, which we define as

$$v_{n,\mathrm{corr},a}(\Delta t_a) = \frac{1}{2X_{\mathrm{dc}}} i_{sa}(t) \Delta s_a \Delta t_a\,. \tag{11}$$

Modifying the switching transition by Δt_a changes the phase a contribution of the NP potential by $v_{n,\mathrm{corr},a}(\Delta t_a)$.

In a next step, we generalize the NP potential correction to three phases and to an arbitrary number of switching transitions. Assume that n_x switching transitions are located within the time interval $[t\ t_1]$ in phase x. As before, assume that the phase currents are constant within $[t\ t_1]$. This leads to the correction of the NP potential

$$v_{n,\mathrm{corr}}(\Delta \boldsymbol{t}) = \frac{1}{2X_{\mathrm{dc}}} \Big(i_{sa}(t) \sum_{i=1}^{n_a} \Delta s_{ai} \Delta t_{ai} + i_{sb}(t) \sum_{i=1}^{n_b} \Delta s_{bi} \Delta t_{bi} + i_{sc}(t) \sum_{i=1}^{n_c} \Delta s_{ci} \Delta t_{ci} \Big)\,, \tag{12}$$

which is a function of the phase currents, switching transitions and modifications to the switching instants

$$\Delta t_{xi} = t_{xi} - t_{xi}^*\,. \tag{13}$$

Recall that t_{xi}^* denotes the nominal switching instant of the ith switching transition in phase x, and t_{xi}

refers to the modified switching instant. The switching instant modifications can be aggregated in the vector

$$\Delta \boldsymbol{t} = [\Delta t_{a1}\ \Delta t_{a2} \ldots \Delta t_{an_a}\ \Delta t_{b1} \ldots \Delta t_{bn_b}\ \Delta t_{c1} \ldots \Delta t_{cn_c}]^T\,, \tag{14}$$

which is of the dimension $n = n_a + n_b + n_c$. Equation (12) can then be stated as the scalar product

$$v_{n,\mathrm{corr}}(\Delta \boldsymbol{t}) = -\boldsymbol{w}^T \Delta \boldsymbol{t}\,, \tag{15}$$

where $\boldsymbol{w} = -\frac{1}{2X_{\mathrm{dc}}}\left[i_{sa}\Delta s_{a1}\ i_{sa}\Delta s_{a2}\ \ldots i_{sa}\Delta s_{an_a}\ i_{sb}\Delta s_{b1}\ \ldots i_{sb}\Delta s_{bn_b}\ i_{sc}\Delta s_{c1}\ \ldots i_{sc}\Delta s_{cn_c}\right]^T$. Note that $\boldsymbol{w}$ is a time-varying vector; we dropped the time dependency from the phase currents to simplify the notation.

MP^{3}C with Integrated Balancing of the NP Potential

The electromagnetic torque and magnetization of an electrical machine can be controlled by regulating its stator flux vector along a given reference trajectory. As shown in [15], this concept can be extended to OPPs. By integrating over time the switched voltage waveform of the OPP, the optimal stator flux reference trajectory in stationary orthogonal αβ coordinates can be obtained. By closely tracking this reference trajectory, minimal current distortions are achieved in the presence of dc-link voltage fluctuations and inverter non-idealities.

As a generalization of [15], the stator flux control problem was formulated in [4] as a model predictive control (MPC) problem with a receding horizon policy, to which we refer as model predictive pulse pattern control (MP^{3}C). The control objectives are mapped into a cost function over a finite prediction horizon of length $T_p = t_1 - t$. A penalty term in the cost function controls the stator flux vector $\boldsymbol{\psi}_s$ along its optimal trajectory in the αβ plane. The stator flux error is defined as

$$\boldsymbol{\psi}_{s,\mathrm{err}} = \boldsymbol{\psi}_s^* - \boldsymbol{\psi}_s\,. \tag{16}$$

The stator flux error at the end of the prediction horizon at time $t + T_p$ can be controlled close to zero by manipulating the switching instants of the switching transitions within the horizon T_p. For an in-depth introduction to MP^{3}C, the interested reader is referred to [4] and [16, Chapter 12].

To address the balancing of the NP potential in MP^{3}C, we define the extended cost function

$$J(\Delta \boldsymbol{t}) = \left\|\boldsymbol{\psi}_{s,\mathrm{err}} - \boldsymbol{\psi}_{s,\mathrm{corr}}(\Delta \boldsymbol{t})\right\|_2^2 + \lambda_v \left(v_{n,\mathrm{err}} - v_{n,\mathrm{corr}}(\Delta \boldsymbol{t})\right)^2 + \lambda_u \left\|\Delta \boldsymbol{t}\right\|_2^2\,, \tag{17}$$

which consists of three terms. The first term penalizes the difference between the stator flux error at time t, which is given by (16), and the corrections made to the stator flux over the time interval $[t\ t + T_p]$. The difference between these two quantities is the uncorrected stator flux error at the end of the prediction horizon at time $t + T_p$. This uncorrected error is penalized using a quadratic penalty, where $\|\boldsymbol{\xi}\|_2^2 = \boldsymbol{\xi}^T\boldsymbol{\xi}$ and $\boldsymbol{\xi}$ is a vector. As shown in [4], the stator flux correction in αβ as a function of the modifications $\Delta \boldsymbol{t}$ of the switching time instants can be written as

$$\boldsymbol{\psi}_{s,\mathrm{corr}}(\Delta \boldsymbol{t}) = -\frac{v_{\mathrm{dc}}}{2}\boldsymbol{K}\begin{bmatrix} \sum_{i=1}^{n_a} \Delta u_{ai}\Delta t_{ai} \\ \sum_{i=1}^{n_b} \Delta u_{bi}\Delta t_{bi} \\ \sum_{i=1}^{n_c} \Delta u_{ci}\Delta t_{ci} \end{bmatrix}\,, \tag{18}$$

where $\boldsymbol{K}$ is the (amplitude-invariant) Clarke transformation from the three-phase *abc* system to the stationary and orthogonal αβ coordinate system. The integer variable Δu_{xi} denotes the ith single-phase switching transition in phase x.

The second term in (17) penalizes the difference between the error in the NP potential at time t, $v_{n,\mathrm{err}}(t) = v_n^*(t) - v_n(t)$, and the corrections $v_{n,\mathrm{corr}}(\Delta \boldsymbol{t})$ made to the NP potential from time t to $t + T_p$. The quantity $v_n^*(t)$ denotes the reference of the NP potential, which is typically zero. The trade-off between stator flux tracking and NP potential balancing is adjusted by the non-negative scalar penalty λ_v.

The third term in the cost function penalizes modifications to the switching instants $\Delta\boldsymbol{t}$. This is done using the quadratic term $\Delta\boldsymbol{t}^T\Delta\boldsymbol{t}$ and the non-negative penalty weight λ_u, which is typically very small.

The switching instants cannot be modified arbitrarily. Constraints are imposed in each phase that limit the switching instants in two ways. First, the current time instant $t = kT_s$, where $k \in \mathbb{N}$ is the current time step and T_s is the sampling interval, is imposed as a lower bound to ensure that switching transitions are not moved into the past. Second, the time instants of the neighboring switching transitions in the same phase are imposed as lower and upper constraints, thus ensuring that the correct sequence of switching transitions is kept.

Minimizing the cost function (17) subject to these constraints leads to the optimization problem

$$\underset{\Delta\boldsymbol{t}}{\text{minimize}}\ J(\Delta\boldsymbol{t}) \tag{19a}$$

$$\text{subject to}\ \ kT_s \le t_{a1} \le t_{a2} \le \ldots \le t_{an_a} \le t^*_{a(n_a+1)} \tag{19b}$$

$$kT_s \le t_{b1} \le t_{b2} \le \ldots \le t_{bn_b} \le t^*_{b(n_b+1)} \tag{19c}$$

$$kT_s \le t_{c1} \le t_{c2} \le \ldots \le t_{cn_c} \le t^*_{c(n_c+1)}\,. \tag{19d}$$

Recall that n_a, n_b and n_c denote the number of switching transitions within the prediction horizon of the three phases. The parameter $t^*_{a(n_a+1)}$ refers to the first nominal switching transition in phase a beyond the horizon. The quantities for phases b and c are defined accordingly.

Cost Function in Vector Format

To solve (19), we need to explicitly state the optimization problem in terms of the optimization or decision vector. In our case, this is the vector of switching instant modifications $\Delta\boldsymbol{t}$. To do so, we rewrite the first term in (17) as $J_1(\Delta\boldsymbol{t}) = \left\|\boldsymbol{\psi}_{s,\mathrm{err}} + \boldsymbol{W}\Delta\boldsymbol{t}\right\|_2^2$ with

$$\boldsymbol{W} = \frac{v_{\mathrm{dc}}}{6}\begin{bmatrix} 2\Delta u_{a1} & \ldots & 2\Delta u_{an_a} & -\Delta u_{b1} & \ldots & -\Delta u_{bn_b} & -\Delta u_{c1} & \ldots & -\Delta u_{cn_c} \\ 0 & \ldots & 0 & \sqrt{3}\Delta u_{b1} & \ldots & \sqrt{3}\Delta u_{bn_b} & -\sqrt{3}\Delta u_{c1} & \ldots & -\sqrt{3}\Delta u_{cn_c} \end{bmatrix}. \tag{20}$$

According to (15), the second term in (17) directly follows to $J_2(\Delta\boldsymbol{t}) = \lambda_v\left(v_{n,\mathrm{err}} + \boldsymbol{w}^T\Delta\boldsymbol{t}\right)^2$. With these definitions, we can rewrite the cost function (17) as

$$J(\Delta\boldsymbol{t}) = J_1(\Delta\boldsymbol{t}) + J_2(\Delta\boldsymbol{t}) + \lambda_u\Delta\boldsymbol{t}^T\Delta\boldsymbol{t} = \left\|\begin{bmatrix}\boldsymbol{\psi}_{s,\mathrm{err}} + \boldsymbol{W}\Delta\boldsymbol{t} \\ v_{n,\mathrm{err}} + \boldsymbol{w}^T\Delta\boldsymbol{t}\end{bmatrix}\right\|_{\boldsymbol{Q}}^2 + \lambda_u\Delta\boldsymbol{t}^T\Delta\boldsymbol{t}\,, \tag{21}$$

where $\|\boldsymbol{\xi}\|_{\boldsymbol{Q}}^2 = \boldsymbol{\xi}^T\boldsymbol{Q}\boldsymbol{\xi}$ and $\boldsymbol{Q} = \mathrm{diag}([1\ 1\ \lambda_v])$. We define the output error vector $\boldsymbol{y}_{\mathrm{err}}$ and matrix $\boldsymbol{V}$ as

$$\boldsymbol{y}_{\mathrm{err}} = \begin{bmatrix}\boldsymbol{\psi}_{s,\mathrm{err}} \\ v_{n,\mathrm{err}}\end{bmatrix}\ \text{ and }\ \boldsymbol{V} = \begin{bmatrix}\boldsymbol{W} \\ \boldsymbol{w}^T\end{bmatrix}, \tag{22}$$

respectively. This allows us to write the cost function (21) in the compact form

$$J(\Delta\boldsymbol{t}) = \|\boldsymbol{y}_{\mathrm{err}} + \boldsymbol{V}\Delta\boldsymbol{t}\|_{\boldsymbol{Q}}^2 + \lambda_u\Delta\boldsymbol{t}^T\Delta\boldsymbol{t}\,, \tag{23}$$

which can be expanded to $J(\Delta\boldsymbol{t}) = (\boldsymbol{y}_{\mathrm{err}} + \boldsymbol{V}\Delta\boldsymbol{t})^T\boldsymbol{Q}(\boldsymbol{y}_{\mathrm{err}} + \boldsymbol{V}\Delta\boldsymbol{t}) + \lambda_u\Delta\boldsymbol{t}^T\Delta\boldsymbol{t}$. By completing the squares, this expression can be further simplified to

$$J(\Delta\boldsymbol{t}) = \Delta\boldsymbol{t}^T(\boldsymbol{V}^T\boldsymbol{Q}\boldsymbol{V} + \lambda_u\boldsymbol{I})\Delta\boldsymbol{t} + 2\boldsymbol{y}_{\mathrm{err}}^T\boldsymbol{Q}\boldsymbol{V}\Delta\boldsymbol{t} + \boldsymbol{y}_{\mathrm{err}}^T\boldsymbol{Q}\boldsymbol{y}_{\mathrm{err}}\,, \tag{24}$$

where we have introduced the $n \times n$ identity matrix $\boldsymbol{I}$. With the definitions

$$\boldsymbol{H} = 2\boldsymbol{V}^T\boldsymbol{Q}\boldsymbol{V} + \lambda_u\boldsymbol{I}\ \text{ and }\ \boldsymbol{c} = 2\boldsymbol{V}^T\boldsymbol{Q}^T\boldsymbol{y}_{\mathrm{err}}\,, \tag{25}$$

and by neglecting the constant offset term $\boldsymbol{y}_{\text{err}}^T \boldsymbol{Q} \boldsymbol{y}_{\text{err}}$ in (24), the cost function can be written in the canonical form $J(\Delta \boldsymbol{t}) = 0.5 \Delta \boldsymbol{t}^T \boldsymbol{H} \Delta \boldsymbol{t} + \boldsymbol{c}^T \Delta \boldsymbol{t}$.

Constraints in Vector Format

We also need to state the constraints on the switching instants in terms of the decision vector. With the definition (13), it is straightforward to rewrite the constraints (19b) on the switching instants for phase a in matrix form. This results in

$$\boldsymbol{G}_a \Delta \boldsymbol{t}_a \leq \boldsymbol{g}_a \tag{26}$$

with

$$\boldsymbol{G}_a = \begin{bmatrix} -1 & 0 & \dots & & & \\ 1 & -1 & 0 & \dots & & \\ 0 & 1 & -1 & 0 & \dots & \\ & \ddots & \ddots & \ddots & \ddots & \\ & \dots & 0 & 1 & -1 & 0 \\ & & \dots & 0 & 1 & -1 \\ & & & \dots & 0 & 1 \end{bmatrix} \text{ and } \boldsymbol{g}_a = \begin{bmatrix} t_{a1}^* - kT_s \\ t_{a2}^* - t_{a1}^* \\ t_{a3}^* - t_{a2}^* \\ \vdots \\ t_{a(n_a-1)}^* - t_{a(n_a-2)}^* \\ t_{an_a}^* - t_{a(n_a-1)}^* \\ t_{a(n_a+1)}^* - t_{an_a}^* \end{bmatrix}. \tag{27}$$

$\boldsymbol{G}_a$ is of dimension $(n_a+1) \times n_a$, whereas $\boldsymbol{g}_a$ is a row vector of length n_a. The vector of switching time modifications in phase a, $\Delta \boldsymbol{t}_a = [\Delta t_{a1}\ \Delta t_{a2} \dots \Delta t_{an_a}]^T$, is defined in accordance with (14).

Similarly, the constraints associated with phases b and c, (19c) and (19d), can be expressed by

$$\boldsymbol{G}_b \Delta \boldsymbol{t}_b \leq \boldsymbol{g}_b \tag{28a}$$

$$\boldsymbol{G}_c \Delta \boldsymbol{t}_c \leq \boldsymbol{g}_c\,. \tag{28b}$$

Their matrices $\boldsymbol{G}_b$, $\boldsymbol{G}_c$ and vectors $\boldsymbol{g}_b$, $\boldsymbol{g}_c$ are defined according to (27). The single-phase constraints (26) and (28) can then be aggregated to the three-phase constraint $\boldsymbol{G} \Delta \boldsymbol{t} \leq \boldsymbol{g}$ with

$$\boldsymbol{G} = \begin{bmatrix} \boldsymbol{G}_a & \boldsymbol{0} & \boldsymbol{0} \\ \boldsymbol{0} & \boldsymbol{G}_b & \boldsymbol{0} \\ \boldsymbol{0} & \boldsymbol{0} & \boldsymbol{G}_c \end{bmatrix} \text{ and } \boldsymbol{g} = \begin{bmatrix} \boldsymbol{g}_a \\ \boldsymbol{g}_b \\ \boldsymbol{g}_c \end{bmatrix}, \tag{29}$$

where $\boldsymbol{0}$ denotes zero matrices of appropriate dimensions.

Quadratic Program

This leads to the quadratic program (QP)

$$\underset{\Delta \boldsymbol{t}}{\text{minimize}}\ \frac{1}{2} \Delta \boldsymbol{t}^T \boldsymbol{H} \Delta \boldsymbol{t} + \boldsymbol{c}^T \Delta \boldsymbol{t} \tag{30a}$$

$$\text{subject to } \boldsymbol{G} \Delta \boldsymbol{t} \leq \boldsymbol{g}\,. \tag{30b}$$

in the decision vector $\Delta \boldsymbol{t}$. Compared with the original MP^{3}C formulation without integrated balancing of the NP potential, the dimension of the QP remains the same; this implies that the computational burden to solve the QP is similar. To solve the QP in real time, a gradient-based solver on a field-programmable gate array (FPGA) is recommended. As proposed in [17], the QP can be reformulated as a constant-size problem and recast as a dual problem. Using an efficient projection method onto the feasible set imposed by the constraints (30b), a tailored and highly resource-efficient QP solver results. In particular, the computation time is about $10\,\mu$s on an FPGA when considering at most nine switching transitions within the prediction horizon.

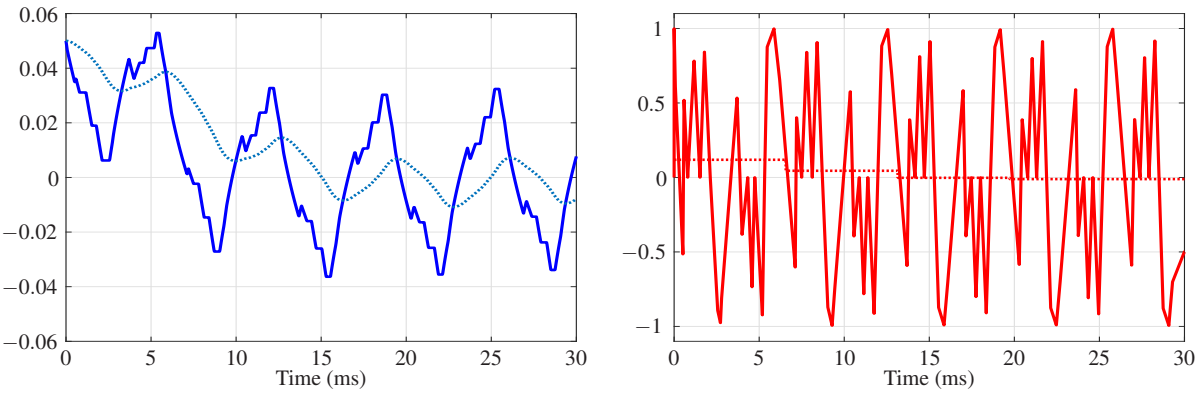

(a) NP potential v_n (solid line) and low-pass filtered NP potential (dotted line) in pu

(b) NP current i_n (solid line) and average NP current over one third of the fundamental period (dotted line) in pu

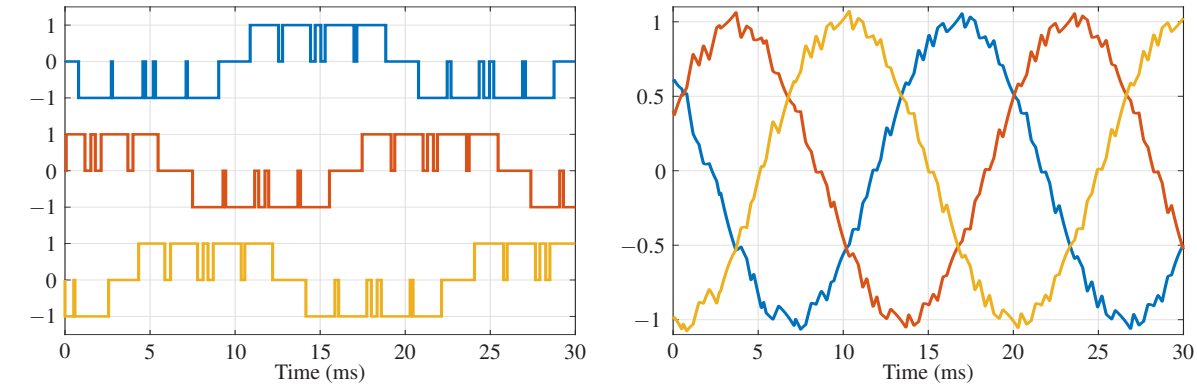

(c) Three-phase switch position

(d) Three-phase stator current in pu

Fig. 3: Control of the NP potential at nominal speed and rated torque

Performance Evaluation

To illustrate the effectiveness of the proposed approach, consider an NPC voltage source inverter connected to a medium-voltage (MV) induction machine and a constant mechanical load. A 3.3 kV and 50 Hz squirrel-cage induction machine rated at 2 MVA with a total leakage reactance of 0.25 pu is used as an example of a typical MV induction machine. The per unit (pu) system is established using the base quantities $V_B = \sqrt{2/3}V_{\text{rat}} = 2694\,\text{V}$, $I_B = \sqrt{2}I_{\text{rat}} = 503.5\,\text{A}$ and $f_B = f_{\text{rat}} = 50\,\text{Hz}$, with V_{rat}, I_{rat} and f_{rat} referring to the rated voltage, current and frequency, respectively. The total dc-link voltage is $v_{\text{dc}} = 5.2\,\text{kV}$, and each dc-link capacitor is $X_{\text{dc}} = 3.36$ pu.

Regarding the control parameters of MP^{3}C, the length of the prediction horizon is chosen as 1/12 of the fundamental period, i.e., as 30°. The penalty on the NP potential error is set to $\lambda_n = 0.015$. Larger penalties result in a more aggressive balancing of the NP potential, whereas smaller penalties slow down the balancing. The penalty on modifying the switching transitions is chosen as $\lambda_u = 0.001$; it is, thus, very small. Recall that our control objective is to remove any dc-offset from the NP potential; its ripple, however, is a characteristic of the OPP and the phase current. To avoid interfering with the optimality of the OPP, possibly increasing the current distortions, it is preferable to not modify this ripple. We therefore apply a low-pass filter to the measured NP potential, whose cut-off frequency is equal to the fundamental frequency.

Consider operation of the drive at nominal speed and rated torque. An idealized Matlab simulation is used in which measurement and computation delays, deadtimes, measurement noise, flux observer errors, parameter variations, dc-link voltage ripple and saturation of the machine's magnetic material are neglected. An OPP with pulse number $d = 5$ is chosen, which results in a device switching frequency of 250 Hz. The initial value of the NP potential is offset from zero and set to $v_n = 0.05$ pu; its reference is

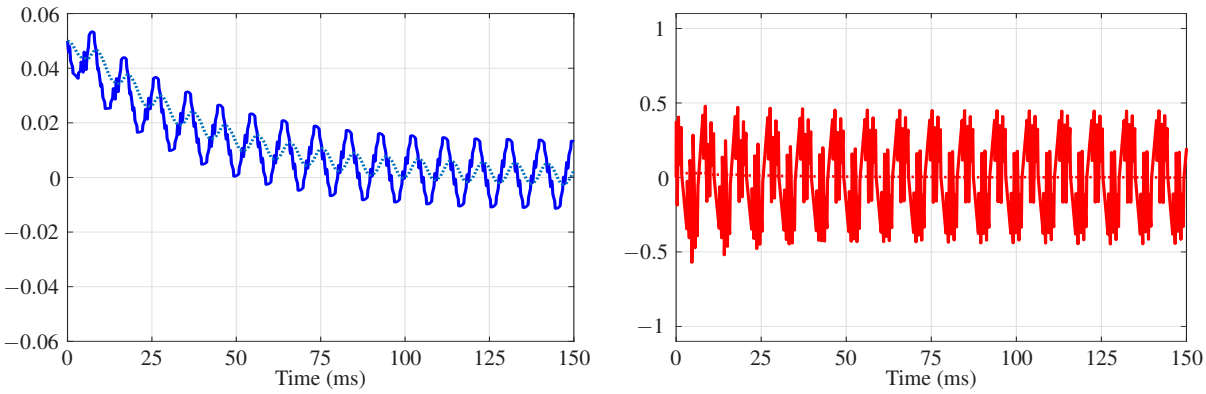

(a) NP potential v_n (solid line) and low-pass filtered NP potential (dotted line) in pu

(b) NP current i_n (solid line) and average NP current over one third of the fundamental period (dotted line) in pu

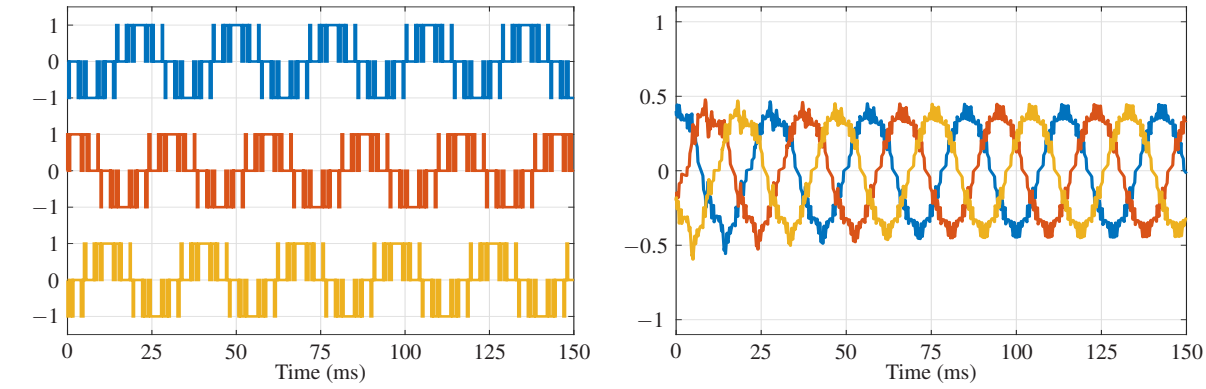

(c) Three-phase switch position

(d) Three-phase stator current in pu

Fig. 4: Control of the NP potential at 0.7 pu speed and zero torque

zero. When setting λ_n to zero, thus disabling the balancing of the NP potential, the NP potential drifts away at a rate of about 0.03 pu per 100 ms. It is, thus, unstable at this operating point.

Fig. 3 shows the simulated response of the MP^{3}C scheme with active NP balancing ($\lambda_n = 0.015$) over 1.5 fundamental periods. Specifically, Fig. 3(a) shows the evolution of the NP potential along with the low-pass filtered version. The offset of the NP potential is removed within less than one fundamental period by effectively adding a negative common-mode component to the switch positions, which injects a positive NP current component. The latter is shown in Fig. 3(b) as solid line; the dash-dotted line refers to the average NP current over one third of the fundamental period. The three-phase switch positions and the stator currents of the machine are shown in Figs. 3(c) and 3(d), respectively.

To control the NP potential to zero only minor modifications to the switching instants are required in the order of a few microseconds. These modifications produce a dc-component in the common-mode voltage, similar to traditional NP potential balancing methods for CB-PWM or SVM. As the common-mode voltage does not drive a differential-mode current, the fundamental component of the stator currents remains unchanged. However, the balancing method slightly alters the ripple of the phase currents, which might increase the current distortions. Across varying operating points, this increase is usually negligible and limited to transients with large offsets in the NP potential.

Another simulation was run at 70% speed and zero torque. The pulse number was increased to $d = 7$, giving a device switching frequency of 245 Hz. An initial offset of 0.05 pu was again investigated for the NP potential. The open-loop response of the NP potential (with $\lambda_n = 0$) is now stable, i.e. natural balancing is effective [6]. Fig. 4 shows closed-loop simulation results for MP^{3}C with $\lambda_n = 0.015$. NP balancing is very slow and only marginally faster than natural balancing. This is to be expected; the principle of injecting a common-mode component is ineffective at zero torque operation, in which the

phase currents and phase voltages are 90° phase-shifted, see also [8]. By modulating the phase current ripple, see the first 50 ms in Fig. 4(d), MP^{3}C nevertheless achieves some active balancing of the NP potential. Crucially, MP^{3}C does not destabilize the NP potential.

Nevertheless, an alternative balancing method should be considered at low power factors, such as redundant voltage vectors; these were proposed in [11] and generalized in [13]. Redundant voltage vectors are easy to implement and provide an almost instantaneous balancing action.

Conclusions

MP^{3}C with OPPs was extended to include the balancing of the NP potential in NPC inverters. Stator flux trajectory control and NP balancing are treated in a single control loop by modifying the switching instants of the OPP. In case of large deviations of the NP potential from zero, NP balancing is prioritized in the cost function, possibly by modifying the current ripple. The fundamental stator flux component nevertheless accurately tracks its reference, ensuring that the desired torque and machine magnetization are achieved. When the NP potential is close to zero, MP^{3}C prioritizes tracking of the stator flux trajectory; this ensures that the optimal current ripple of the OPP is achieved, thus minimizing the current distortions.

References

[1] H. S. Patel and R. G. Hoft, "Generalized techniques of harmonic elimination and voltage control in thyristor inverters: Part I–Harmonic elimination," *IEEE Trans. Ind. Appl.*, vol. IA-9, pp. 310–317, May/Jun. 1973.

[2] G. S. Buja, "Optimum output waveforms in PWM inverters," *IEEE Trans. Ind. Appl.*, vol. 16, pp. 830–836, Nov./Dec. 1980.

[3] B. Beyer, *Schnelle Stromregelung für Hochleistungsantriebe mit Vorgabe der Stromtrajektorie durch off-line optimierte Pulsmuster*. PhD thesis, Wuppertal University, 1998.

[4] T. Geyer, N. Oikonomou, G. Papafotiou, and F. Kieferndorf, "Model predictive pulse pattern control," *IEEE Trans. Ind. Appl.*, vol. 48, pp. 663–676, Mar./Apr. 2012.

[5] T. Geyer and N. Oikonomou, "Model predictive pulse pattern control with very fast transient responses," in *Proc. IEEE Energy Convers. Congr. Expo.*, (Pittsburgh, PA, USA), Sep. 2014.

[6] H. du Toit Mouton, "Natural balancing of three-level neutral-point-clamped PWM inverters," *IEEE Trans. Ind. Electron.*, vol. 49, pp. 1017–1025, Oct. 2002.

[7] S. Ogasawara and H. Akagi, "Analysis of variation of neutral point potential in neutral-point-clamped voltage source PWM inverters," in *Proc. IEEE Ind. Appl. Soc. Annu. Mtg.*, Oct. 1993.

[8] C. Newton and M. Sumner, "Neutral point control for multi-level inverters: Theory, design and operational limitations," in *Proc. IEEE Ind. Appl. Soc. Annu. Mtg.*, Oct. 1997.

[9] J. K. Steinke, "Switching frequency optimal PWM control of a three-level inverter," *IEEE Trans. Power Electron.*, vol. 7, pp. 487–496, Jul. 1992.

[10] M. Sprenger, R. Alvarez, and S. Bernet, "Direct dead-time control — A novel DC-link neutral-point balancing method for the three-level neutral-point-clamped voltage source inverter," in *Proc. IEEE Energy Convers. Congr. Expo.*, (Raleigh, NC, USA), pp. 1157–1163, Sep. 2012.

[11] J. Pou, R. Pinando, D. Borojevich, and P. Rodríguez, "Evaluation of the low-frequency neutral-point voltage oscillations in the three-level inverter," *IEEE Trans. Ind. Electron.*, vol. 52, pp. 1582–1588, Dec. 2005.

[12] T. Brückner and D. G. Holmes, "Optimal pulse-width modulation for three-level inverters," *IEEE Trans. Power Electron.*, vol. 20, pp. 82–89, Jan. 2005.

[13] J. Holtz and N. Oikonomou, "Neutral point potential balancing algorithm at low modulation index for three-level inverter medium-voltage drives," *IEEE Trans. Ind. Appl.*, vol. 43, pp. 761–768, May/Jun. 2007.

[14] T. Boller, J. Holtz, and A. K. Rathore, "Neutral-point potential balancing using synchronous optimal pulsewidth modulation of multilevel inverters in medium-voltage high-power AC drives," *IEEE Trans. Ind. Appl.*, vol. 50, pp. 549–557, Jan./Feb. 2014.

[15] J. Holtz and N. Oikonomou, "Synchronous optimal pulsewidth modulation and stator flux trajectory control for medium-voltage drives," *IEEE Trans. Ind. Appl.*, vol. 43, pp. 600–608, Mar./Apr. 2007.

[16] T. Geyer, *Model predictive control of high power converters and industrial drives*. London, UK: Wiley, Oct. 2016.

[17] S. Richter, T. Geyer, and M. Morari, "Resource-efficient gradient methods for model predictive pulse pattern control on an FPGA," *IEEE Trans. Contr. Syst. Technol.*, vol. 25, pp. 828–841, May 2017.